

Gaia uncovers difference in B and Be star binarity at small scales: evidence for mass transfer causing the Be phenomenon

Jonathan M. Dodd,¹★ René D. Oudmaijer,¹ Isaac C. Radley,¹ Miguel Vioque^{2,3} and Abigail J. Frost^{4,5}

¹*School of Physics and Astronomy, University of Leeds, Woodhouse Lane, Leeds LS2 9JT, UK*

²*Joint ALMA Observatory, Alonso de Córdova 3107, Vitacura, Santiago 763-0355, Chile*

³*National Radio Astronomy Observatory, 520 Edgemont Road, Charlottesville, VA 22903, USA*

⁴*Institute of Astronomy, KU Leuven, Celestijnlaan 200D, B-3001 Leuven, Belgium*

⁵*European Southern Observatory (ESO), Alonso de Córdova 3107, Vitacura, Santiago 763-0355, Chile*

Accepted 2023 October 5. Received 2023 October 5; in original form 2023 June 2

ABSTRACT

Be stars make up almost 20 percent of the B star population, and are rapidly rotating stars surrounded by a disc; however the origin of this rotation remains unclear. Mass transfer within close binaries provides the leading hypothesis, with previous detections of stripped companions to Be stars supporting this. Here, we exploit the exquisite astrometric precision of *Gaia* to carry out the largest to date comparative study into the binarity of matched samples of nearby B and Be stars from the Bright Star Catalogue. By utilizing new ‘proper motion anomaly’ values, derived from *Gaia* DR2 and DR3 astrometric data alongside previous values calculated using *Hipparcos* and *Gaia* data, and the *Gaia*-provided RUWE, we demonstrate that we can identify unresolved binaries down to separations of 0.02 arcsec. Using these measures, we find that the binary fractions of B and Be stars are similar between 0.04 and 10 arcsec, but the Be binary fraction is significantly lower than that of the B stars for separations below 0.04 arcsec. As the separation range of these ‘missing’ binaries is too large for mass transfer, and stripped companions are not retrieved by these measures, we suggest the companions migrate inwards via binary hardening within a triple system. This confirms statistically for the first time the hypothesis that binary interaction causes the Be phenomenon, with migration causing the dearth of Be binaries between 0.02 and 0.04 arcsec. Furthermore, we suggest that triplicity plays a vital role in this migration, and thus in the formation of Be stars as a whole.

Key words: proper motions – binaries: close – stars: emission-line, Be.

1 INTRODUCTION

Be stars make up around 20 percent of the total population of B-type stars (Bodensteiner, Shenar & Sana 2020a) and are defined, in part, by the presence of Balmer emission lines. These lines are thought to originate from a slowly outflowing ionized circumstellar gas-disc (Porter & Rivinius 2003; Rivinius, Carciofi & Martayan 2013; Jones et al. 2022). While the dynamics of these discs have been studied extensively (Wisniewski et al. 2010; Draper et al. 2014; Suffak, Jones & Carciofi 2022), the mechanism by which they form is undetermined. Consensus suggests that the formation is related to the rapid rotation observed in practically the entire Be population (Zorec et al. 2016, 2017), and which is suggested to be at or near the critical velocities of such stars (Townsend, Owocki & Howarth 2004; Granada et al. 2013). Such rapid rotation could thus allow for processes such as turbulence (Townsend, Owocki & Howarth 2004) or non-radial pulsations (Owocki & Cranmer 2002; Semaan et al. 2018) to contribute significantly to the formation of the decretion discs around Be stars due to decreased effective gravity at the surface of such stars (Granada et al. 2013). This, however, only

leads to a further question – what exactly causes Be stars to rapidly rotate?

Three mechanisms have been suggested as the origin of this characteristic rotation: it could be a relic from the parent molecular cloud, the rotation thus a result of inherited angular momentum (Bodenheimer 1995); the envelope of the star could be spun up via momentum transport from a contracting core (Granada et al. 2013; Hastings, Wang & Langer 2020); or, crucially for this study, it could be a result of mass and angular momentum transfer via binary interaction (Shao & Li 2014; Bodensteiner, Shenar & Sana 2020a).

If binary interaction is the source of this rapid rotation, then one could expect that the binary statistics of B and Be stars will differ. This line of reasoning provided the basis for the study performed in Oudmaijer & Parr (2010), which found the binary fraction of B- and Be-type stars to be similar between separations of 0.1 and 8 arcsec based on a sample of 36 B and 37 Be stars, and concluded that binarity, at least at these scales, could not be responsible for all Be stars. However, while a number of studies into the binarity of Be stars exist (Boubert & Evans 2018; Klement et al. 2019; Hastings et al. 2021 and El-Badry et al. 2022, among others) and suggest the stripping of the companion to the Be star as the cause (Han et al. 2002; El-Badry & Quataert 2021; El-Badry et al. 2022; Nazé et al. 2022), very few comparative studies into the binarity of both B- and Be-

* E-mail: py17jd@leeds.ac.uk

type stars exist. The next most recent points of comparison are Abt & Levy (1978) and Abt & Cardona (1984), each from around 40 yr ago, and which similarly conclude that binarity cannot be responsible for the Be phenomenon at the scales they probe. However, Abt & Levy (1978), which utilizes radial velocity variations to detect binarity, suffers from the effects of small sample sizes, while Abt & Cardona (1984) is hampered by inhomogeneous biases as it is, in effect, a review of the then available literature.

With the advent of high-precision astrometric all-sky surveys, we are now able to mitigate these issues and investigate the multiplicity of large samples. Recent studies have employed astrometric data from surveys such as *Hipparcos* (Van Leeuwen 2007) and *Gaia* (Gaia Collaboration 2021) in order to detect binarity in the overall stellar population, both in the case of wide (El-Badry, Rix & Heintz 2021) and close (Kervella et al. 2019; Kervella, Arenou & Thévenin 2022) binaries. The time is thus ripe for such an investigation into the binarity of B and Be stars.

Here, we utilize the proper motion anomaly (PMA), as introduced in Kervella et al. (2019) (see also Brandt 2018), which is a measure of the difference between long- and short-term proper motions of a point source, in order to determine the fractions of B- and Be-type stars in visually unresolved binary systems. Alongside previously determined PMA values from Kervella, Arenou & Thévenin (2022), calculated using *Hipparcos* and *Gaia* DR3 data (a similar catalogue can also be found in Brandt 2021), we use new values, calculated for the first time in this work using a combination of *Gaia* DR2 and DR3 data (Gaia Collaboration 2018, 2023). Using these metrics we probe binary systems with separations between 0.02 and 1.1 arcsec, and with magnitude differences up to 4 mag.

Additionally we utilize the *Gaia*-provided Renormalized Unit Weight Error (RUWE) to further constrain the binary fractions of these two populations (Stassun & Torres 2021). Thus, we are able to bridge the gap in binary separations between, and expand upon previous radial velocity (Abt & Levy 1978) and adaptive optics (Oudmaijer & Parr 2010) studies of these stars. Additionally, by querying a sample over an order of magnitude larger than present in the most recent similar study (Oudmaijer & Parr 2010), this paper provides the largest scale comparative study of B and Be star binarity to date.

This paper is structured as follows: in Section 2 we detail the two binary detection methods used (the PMA and the RUWE), and demonstrate their sensitivities and limitations; in Section 3 we report the results of utilizing these methods on samples of B and Be stars; and in Section 4 we discuss the implications of these newly reported binary fractions on models for the formation of Be stars.

2 METHODS

2.1 Binary detections via PMA

For any binary system we can define two similar variables, the centre of mass, which the two-component stars orbit, and the photocentre, which describes the location of the apparent point source in an unresolved system. In general, the positions of these two points differ, thus the photocentre also orbits the centre of mass – leading to a deviation from the linear proper motion expected for single sources in the case of unresolved binary systems.

This deviation from the expected linear proper motion, referred to as the PMA, $\Delta\mu$, can be detected through a comparison of long- and short-term proper motion measurements (μ_{lt} and μ_{st} , respectively), with the long-term effectively tracing the motion of the centre of mass and the short term tracing the sum of the centre of mass and relative photocentre motions. An illustration of this principle can be

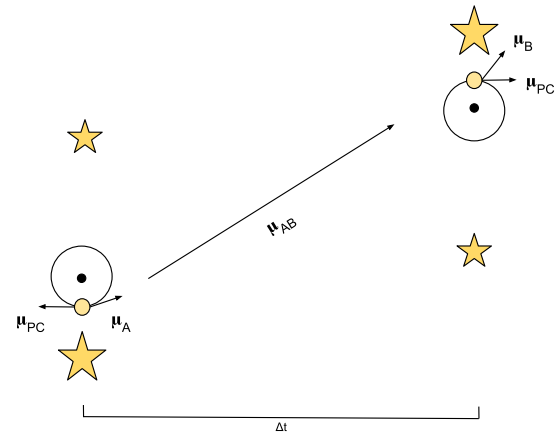


Figure 1. Cartoon illustrating the principle behind the PMA. The large and small stars are the primary and secondary companion, respectively, the black dot is the centre of mass, and the yellow dot the photocentre. Two sets of observations are taken at A and B, with a time interval of Δt between them. μ_A and μ_B are the short-term proper motions measured during their respective observations, and μ_{AB} is the long-term proper motion, determined from the change of observed position over Δt . The arrows labelled μ_{PC} are the instantaneous proper motions of the photocentre in the frame where the centre of mass is stationary.

found in Fig. 1. The PMA can thus be expressed as

$$\Delta\mu = \mu_{st} - \mu_{lt} \quad (1)$$

Due to current advances in the precision of proper motion measurements, alongside high-precision positional measurements allowing for long-term proper motions to be calculated, the PMA thus provides a powerful tool in the search for unresolved binary candidates within large samples of stars.

This measure is sensitive to the period of a given binary system. Periods significantly longer than the time elapsed over the long-term proper motion measurement Δt will have a deviation in proper motion too small to be detected. Similarly, systems wherein a whole number of complete orbits have occurred during the measurement of the long-term proper motion will not be detected, again as the deviation in long- and short-term proper motions will be too small to detect.

Following this logic, peak sensitivity of the PMA should be achieved for systems where an $\frac{2n+1}{2}$ orbital periods have elapsed between the two observations, as the absolute change in orbital phase is at a maximum here. However, in reality, due to the time-window smearing effects present over the observation periods of the two constituent astrometric surveys (Kervella, Arenou & Thévenin 2022) there is a general decrease in sensitivity towards smaller periods, with peak sensitivity being achieved for periods of $P \simeq \Delta t$ (Kervella, Arenou & Thévenin 2022). This also explains why, although of much higher astrometric precision, the DR2-DR3 derived PMA's probe larger periods than the *Hipparcos*-DR3 PMA values (as will be shown in the following section). Next, we will probe the sensitivity limits of the various methods both theoretically and empirically.

2.1.1 Separation limits of the PMA

Although the sensitivity of the PMA to mass as a function of orbital period (and thus linear separation) has previously been investigated (Kervella, Arenou & Thévenin 2022), the sensitivity to angular separation remains unexamined. As detailed in Appendix A, using an idealized theoretical model, consisting of a face-on, circularly

orbiting binary system, we arrive at a minimum detectable separation of 0.01 arcsec for PMA values calculated using *Hipparcos* and *Gaia* DR3 data. Additionally, when considering the PMA calculated using *Gaia* DR2 and DR3 data, the theoretical minimum detectable separation is 0.0025 arcsec. However, this computation does not take into account the effect of the time-window smearing during the PM measurement – which leads to the DR2-DR3 PMA losing out on the shorter separations.

It is thus useful to obtain an empirical value as a point of comparison. In order to evaluate this sensitivity of the PMA to varying separations, we use a sample of binary systems listed in the Washington Double Star (WDS, Mason et al. 2022) catalogue. The WDS contains a compilation of multiple star systems for which at least one measured separation is available within the literature. The sources in the WDS were cross-matched with the list provided in Kervella, Arenou & Thévenin (2022) using the xMatch service provided by CDS, Strasbourg (Pineau et al. 2020). No restrictions on mass or spectral type were placed on the stars within the binaries in order to generate the largest, general sample. Reported higher order multiple systems were then removed for the sake of simplicity, as were any systems with separations greater than 10 arcsec. While the PMA primarily probes the unresolved regime of separations by nature, this 10 arcsec limit was selected in order to ensure that no unpredictable effects were materializing at higher separations.

For the resulting 11 116 unique binary systems, we obtained values of the PMA from the Kervella, Arenou & Thévenin (2022) catalogue [which uses data reported in the *Hipparcos* re-reduction (Van Leeuwen 2007) and the *Gaia* DR3 catalogues, giving $\Delta t \approx 25$ yr] and calculated new values, using data available in the *Gaia* Data Release 2 and Data Release 3 (Gaia Collaboration 2018, 2021; $\Delta t \approx 0.5$ yr). The methodology used in Kervella, Arenou & Thévenin (2022) was utilized for the calculation of these new values, with calibration performed via re-calculating *Hipparcos*–*Gaia* DR3 PMA’s replicating the reported PMA values exactly and reported errors to within a precision of 1 per cent.

The final sample contains 10 283 sources with reported PMA values; note that not all values surpass the binary detection threshold of $S/N > 3$. The majority of these systems had separations reported to a precision of 0.1 arcsec. 316 systems have separations reported as 0 arcsec in the WDS Catalogue (i.e. their separations were below 0.1 arcsec). For each of these systems, higher precision separations were retrieved from supplemental WDS material (Mason et al. 2022). Where orbital solutions had previously been reported, the separation available at the *Gaia* DR3 epoch was used.

Fig. 2 shows the median values of the signal-to-noise ratio for the *Hipparcos*–*Gaia* DR3 PMA for the WDS sample at varying separations. These systems have been placed into bins of width 0.1 arcsec at separations greater than or equal to 0.1 arcsec. At separations below 0.1 arcsec the systems have been placed into 10 bins such that each bin has an equal number of systems within it (approximately 30 per bin). For these bins the mean reported separation of the systems within it is plotted.

Based on the data presented in Fig. 2, it can be seen that for the DR3–*Hipparcos* PMA, there is an increase of SNR towards lower reported separations. On average, this PMA remains above the detection threshold of 3 for all separations between 0.02 and 0.7 arcsec (based on the median values). As a result, 0.02–0.7 arcsec appears to be an empirical range of separations detectable via this PMA; at least half of all WDS binary systems with separations within this range are detected (note that we would not expect for all binaries within this range to be detected due to projection effects). This is in agreement with the calculated theoretical minimum detectable

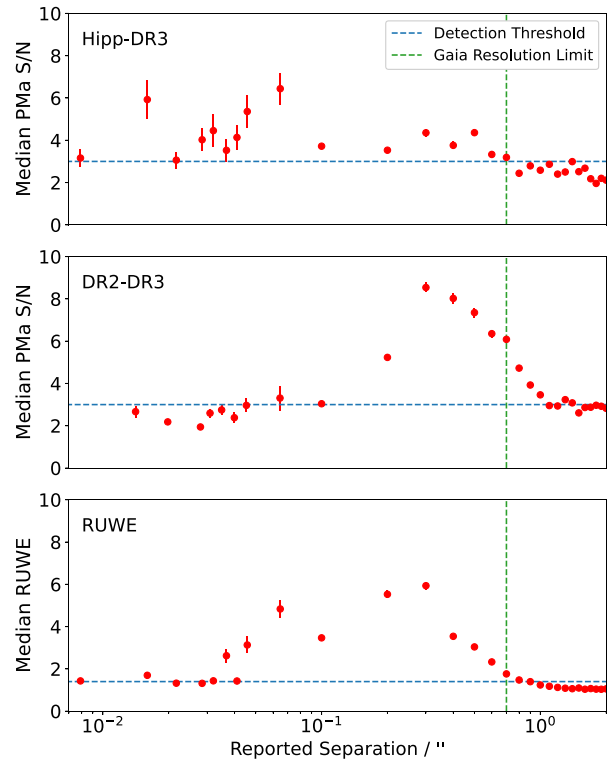


Figure 2. Median values of the *Hipparcos*–*Gaia* DR3 and *Gaia* DR2-DR3 PMA S/N 's and the RUWE, of systems reported as binary in the WDS (Mason et al. 2022). Here, values greater than 3 constitute a detection of binarity by either PMA, and values greater than 1.4 constitute a detection by the RUWE – see Section 2.2 for details.

separation and the expectation that the upper limit occurs somewhere around the spatial resolution limit of the surveys.

It is also to be noted that high PMA systems at separations greater than the resolvable limit (i.e. with separations greater than ~ 1 arcsec) exist in non-negligible numbers. These systems have reported separations much greater than the PMA can detect (as it measures the motion of an essentially unresolved binary), and it is thus likely that they are, in fact, as of yet undetected higher order multiple systems.

Alongside the examination of the Kervella, Arenou & Thévenin (2022) reported *Hipparcos*–*Gaia* DR3 PMA values, an equivalent consideration of *Gaia* DR2-DR3 PMA values has been conducted. As there does not exist an equivalent catalogue as in Kervella, Arenou & Thévenin (2022), these PMA’s were thus calculated via the same process, but using data from the *Gaia* Data Releases 2 and 3.

The median values of these PMA SNR values at a given separation can also be found in Fig. 2. Again, a rise in the median PMA can be seen towards lower separations, here beginning at separations of approximately 1.1 arcsec, increasing towards a peak at around 0.6 arcsec, and remaining above the detection threshold down to 0.2 arcsec. While this lower limit is in disagreement with the theoretical limit of 0.0025 arcsec derived in Appendix A, the theoretical considerations largely ignore the effect of smearing over the observing timeframe. As the DR2-DR3 PMA is smeared across the entirety of the long-term proper motions timeframe, this will mean that the lowest separations are not probed, although the number of potential observable objects increases significantly (as *Gaia* has observed orders or magnitude more objects than *Hipparcos*). Additionally the increase in precision achieved since *Hipparcos* has both resulted

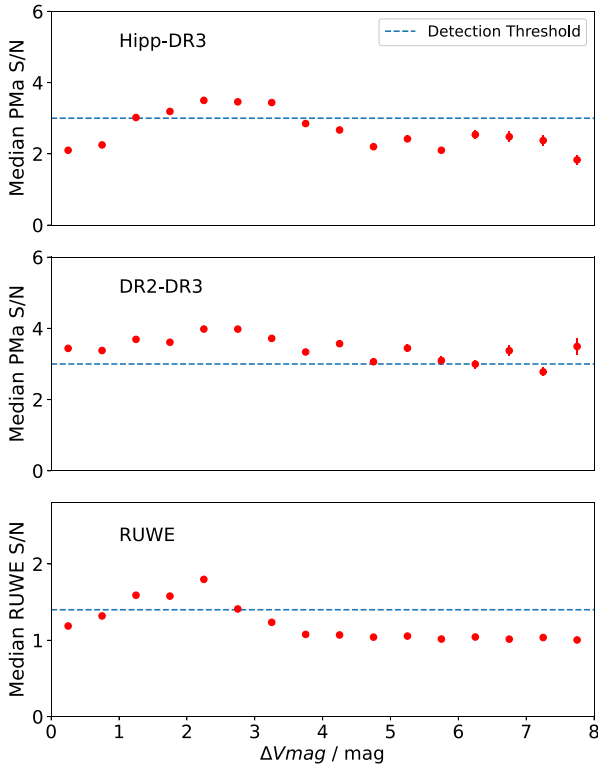


Figure 3. Median PMA of WDS systems, as a function of the difference in magnitude of the two stars for the *Hipparcos–Gaia* DR3 and *Gaia* DR2-DR3 PMA’s and the RUWE. Both plots have been cropped to a maximum difference in magnitude of 8 mag, as the number of systems with magnitude differences greater than this decreases to the point where meaningful conclusions cannot be drawn. Detections are reported out to differences of up to 12 mag in all three cases.

in the upper limit of separations detectable to be expanded beyond the *Gaia* resolution limit, and increased the total fraction of systems detected within the sensitive limit.

These results remain consistent when examining B- and Be-type binaries within the WDS (Mason et al. 2022), with systems within the two sensitive ranges being detected at significantly higher rates than those outside that range.

We thus show that the *Hipparcos–Gaia* DR3 PMA is sensitive to binary systems with angular separations between 0.02–0.7 arcsec, and the *Gaia* DR2-DR3 PMA is sensitive between separations of 0.2–1.1 arcsec.

2.1.2 Magnitude limits of the PMA

In order to evaluate the limitations of the PMA, we must also consider the sensitivity of this measure to the difference in magnitude between the two components. Here, systems contained within the WDS catalogue are once again considered, now limiting the sample to those systems with reported separations between 0 and 1 arcsec in line with the more favourably sensitive range determined in the previous section.

In the case of the *Hipparcos–Gaia* DR3 PMA, and as can be seen in Fig. 3, examining the difference in the WDS reported apparent magnitude reveals that the PMA shows some preferential sensitivity within the 1.0 to 3.5 mag range, peaking at around $\Delta V_{\text{mag}} = 3$ mag.

In the case of the *Gaia* DR2-DR3 PMA, an equivalent examination reveals a general increase in sensitivity across most magnitude differences available via the WDS sample, with the preferentially detected region expanding to systems with a difference in magnitude $0 < \Delta V_{\text{mag}} \leq 4.5$, peaking at around $\Delta V_{\text{mag}} = 2.5$, although significant numbers of detections are still made at greater differences in magnitude.

2.2 Binary detections via the RUWE

The RUWE is a reduced chi-squared parameter that describes the ‘goodness-of-fit’ of a single-body astrometric model to an observed source. As such, it would follow that such a parameter is sensitive to the presence of unresolved binary companions – with the photocentre wobble caused by such a companion causing deviations from what is expected of a single body, resulting in a worse-fitting astrometric solution. Indeed, the RUWE parameter has been suggested to act as a binarity indicator (Belokurov et al. 2020), with values significantly above the normalized value of 1 (i.e. ≥ 1.4 as per Stassun & Torres 2021) being regarded as indicative of the source being ‘badly fit’ by the astrometric solution and thus potentially binary.

Like the PMA, the RUWE varies in sensitivity according to the period of a binary system, with the RUWE having some function of sensitivity to binarity determined both by the period of the system in question and by the time baseline over which the RUWE is determined (approximately 6 months in the case of *Gaia* DR2 and DR3), with Penoyre, Belokurov & Evans (2022) suggesting that for *Gaia* DR3, RUWE is an effective measure of binarity for periods of around a month to a decade.

However, due to sensitivity to other (non-multiplicity related) factors which can inflate the RUWE (Belokurov et al. 2020), it is important to note that there may be some fraction of false positive detections – for example if the sample contains stars known to have circumstellar discs or extended regions of emission (Oudmaijer, Jones & Vioque 2022). This is unlikely to hamper our study of B and Be stars however, as the discs of Be stars are very small when compared to the resolution achieved by *Gaia* DR3 (Quirrenbach et al. 1997; Wheelwright et al. 2012).

2.2.1 Separation limits of the RUWE

The separation limits of the RUWE were determined using the same process as for the PMA above. Here, the detection threshold is given to be 1.4 (as suggested by Stassun & Torres 2021). Based on the data presented in Fig. 2, we find that the RUWE exhibits a sharp and marked increase above the detection threshold at binary separations below the resolution limit of *Gaia* (0.7 arcsec). This increase peaks at approximately 0.09 arcsec, and, on average, remains above the threshold down to separations of 0.04 arcsec. Thus, we find that the RUWE is sensitive to those binary systems with separations ranging between 0.04 and 0.7 arcsec.

2.2.2 Magnitude limits of the RUWE

As with the PMA, it is useful to quantify the sensitivity of the RUWE to the magnitude differences of the binary systems probed. Fig. 3 demonstrates, by repeating the same process as used to determine the magnitude differences the PMA is sensitive to, that it would seem that the RUWE is primarily sensitive to systems with magnitude differences between 1.5 and 3.0 mag, peaking somewhere between 2.0 and 2.5 mag.

Table 1. Populations of main-sequence B- and Be-type stars within the sample, divided by spectral type.

Spectral type	B	Be
B0V	12	4
B1V	47	10
B2V	104	31
B3V	97	19
B4V	31	12
B5V	111	13
B6V	43	8
B7V	48	4
B8V	156	13
B9V	258	9
Total	907	123

We have thus shown that, via these astrometric methods, we can consistently detect visually unresolved binaries with separations as low as 0.04 arcsec using the RUWE, and 0.02 arcsec using the *Hipparcos–Gaia* PMA and with magnitude differences up to 4.5 mag, depending on the measure used. Thus, due to the precision achieved by modern astrometric surveys, we will be able to probe the origins of Be stars with a statistical basis heretofore unavailable.

3 THE BINARITY OF B AND BE STARS

3.1 Sample selection

Here, we utilize the same initial sample of B and Be stars extracted from the Bright Star Catalogue (BSC) fifth Revised Edition (Hoffleit & Jaschek 1991) as used in Radley et al. (in preparation). This sample was then cross-matched within 5 arcsec against the *Gaia* Data Release 3 (Gaia Collaboration 2021) data. Stars without proper motion measurements in the *Hipparcos* or *Gaia* Data Releases were removed. Stars with non-V luminosity classes were also removed in order to ensure that the comparisons made between our two samples are between like sources that are subject to the same selection effects. A summary of the spectral types of the stars included in this sample can be found in Table 1.

This sample provides an almost thirty-fold increase in the number of B-type stars, and a four-fold increase in the number of Be-type stars compared to similar comparative studies (Abt & Levy 1978; Oudmaijer & Parr 2010) that probe a well-defined separation range. Additionally, by virtue of being selected from the same catalogue of the brightest stars in the sky, these stars will be subject to the same selection effects, and have similar brightnesses and parallaxes, thus ensuring their usefulness in comparing how B- and Be-type stars differ in their astrometric properties. These stars are also amongst the most nearby ones, thus allowing us to detect the physically closest companions while remaining within the range of angular separations detectable by our methods (see Sections 2.1.1 and 2.2.1), with the lower end of our detectable range, 0.02 arcsec, equating to 5 au at the mean distance to the stars in these samples.

3.2 Detection of unresolved binaries

We first consider the complete, unmodified samples of 907 B and 123 Be stars, utilizing a combination of PMA values found within the catalogue contained within Kervella, Arenou & Thévenin (2022), calculated using *Hipparcos* and *Gaia* DR3 data, and new PMA values calculated using data reported in *Gaia* Data Releases 2 and 3, as well

as the *Gaia*-provided RUWE. These measures allow us to detect unresolved binary systems via differences in long- and short-term proper motions (for the PMA; see Section 2.1) and via deviations from a single-body astrometric fit (in the case of the RUWE; see Section 2.2).

Using the *Hipparcos–Gaia* DR3 PMA, which probes the range 0.02–0.7 arcsec (see Section 2.1.1), equating to around 5–180 au at the average distance of 260 pc, we arrive at binary fractions of 42 ± 2 per cent and 28 ± 4 per cent for the B and Be samples, respectively.¹ This proves to be a greater than 3σ difference.

In contrast, the *Gaia* DR2-DR3 PMA values reveal similar B and Be binary fractions in the 0.2–1.1 arcsec range (around 50–290 au at 260pc). In this case, the fraction of B stars detected as being in a binary system is found to be 27 ± 1 per cent and the equivalent for Be stars is found to be 29 ± 4 per cent.

Finally, the fractions of B and Be stars detected via applying a detection threshold of $RUWE > 1.4$, tracing binaries with separations between 0.04 and 1.1 arcsec (10–290 au), were found to be 27 ± 1 per cent and 20 ± 4 per cent, respectively. See Table 2 further down for a summary of these binary fractions.

3.3 Correcting biases

Although the global properties of the B and Be stars in the BSC are very similar, the two samples exhibit slightly different properties across a number of observables. For example, by virtue of being rarer, the Be stars are on average further away than the B stars, with the average B star in our sample sitting at a parallax of 5.26 mas with a standard deviation of 3.38 mas, whereas the average Be star sits at a parallax of 3.81 mas with a standard deviation of 2.42 mas. Likewise the average apparent magnitudes of the B and Be populations are 6.06 mag (standard deviation of 1.07 mag) and 5.95 mag (standard deviation of 1.32 mag), respectively. In addition to this, the two populations differ in the distribution of their spectral types (for example, almost 30 per cent of the B stars are B9V, while only 7 per cent of the Be stars are B9Ve). As such, the variations in the distributions of these properties must be taken into account to ensure that the binary fractions are not affected by them.

Thus, in order to remove the effects of these biases, a variety of subsamples of B stars were created. These included random samples, alongside ‘semirandom’ samples wherein the B population was binned according to a given variable, mentioned above, and stars were randomly picked from each bin in order to match the distribution of said variable in the Be sample. In each case a Kolmogorov–Smirnov test was performed in order to confirm that the subsample was likely drawn from the same distribution as the Be population. The binary fraction of each subsample was then determined using the PMA and RUWE detection thresholds detailed above.

A summary of these samples and their binary fractions can be found in Fig. 4. Therein, the greater than 3σ dearth of Be binaries, when compared to the number of B binaries, is still seen to be present at the tightest separations probed by our methods.

3.4 Wider separation binaries

While the focus of this study is on close binaries, we now consider the presence of binary companions outside the 0.02–0.7 arcsec range. Oudmaijer & Parr (2010), who probe separations of

¹Uncertainties here are calculated using the binomial method. Error bars are given at 1σ .

Table 2. Percentage of B and Be stars detected as binary at varying ranges of separations. By utilizing combinations of the previously explored astrometric detection methods we are able to constrain the greater than 3σ dearth of Be binaries to between 0.02 and 0.2 arcsec.

Separation range/ arcsec	B	Be	Detection method
$0.02 \leq x \leq 0.2$	28 ± 1 per cent	17 ± 3 per cent	Detected by the <i>Hipparcos</i> -DR3 PMA but not the DR2-DR3 PMA.
$0.02 \leq x \leq 0.7$	42 ± 2 per cent	28 ± 4 per cent	Detected by the <i>Hipparcos</i> -DR3 PMA.
$0.2 \leq x \leq 1.1$	27 ± 1 per cent	29 ± 4 per cent	Detected by the <i>Gaia</i> DR2-DR3 PMA.
$0.04 \leq x \leq 0.7$	27 ± 1 per cent	20 ± 4 per cent	Detected by the RUWE.
$0.1 \leq x \leq 8$	29 ± 8 per cent	30 ± 8 per cent	Detected by Oudmaijer & Parr (2010)
$0.7 \leq x \leq 10$	6 ± 1 per cent	10 ± 3 per cent	Resolved as binary by <i>Gaia</i> .

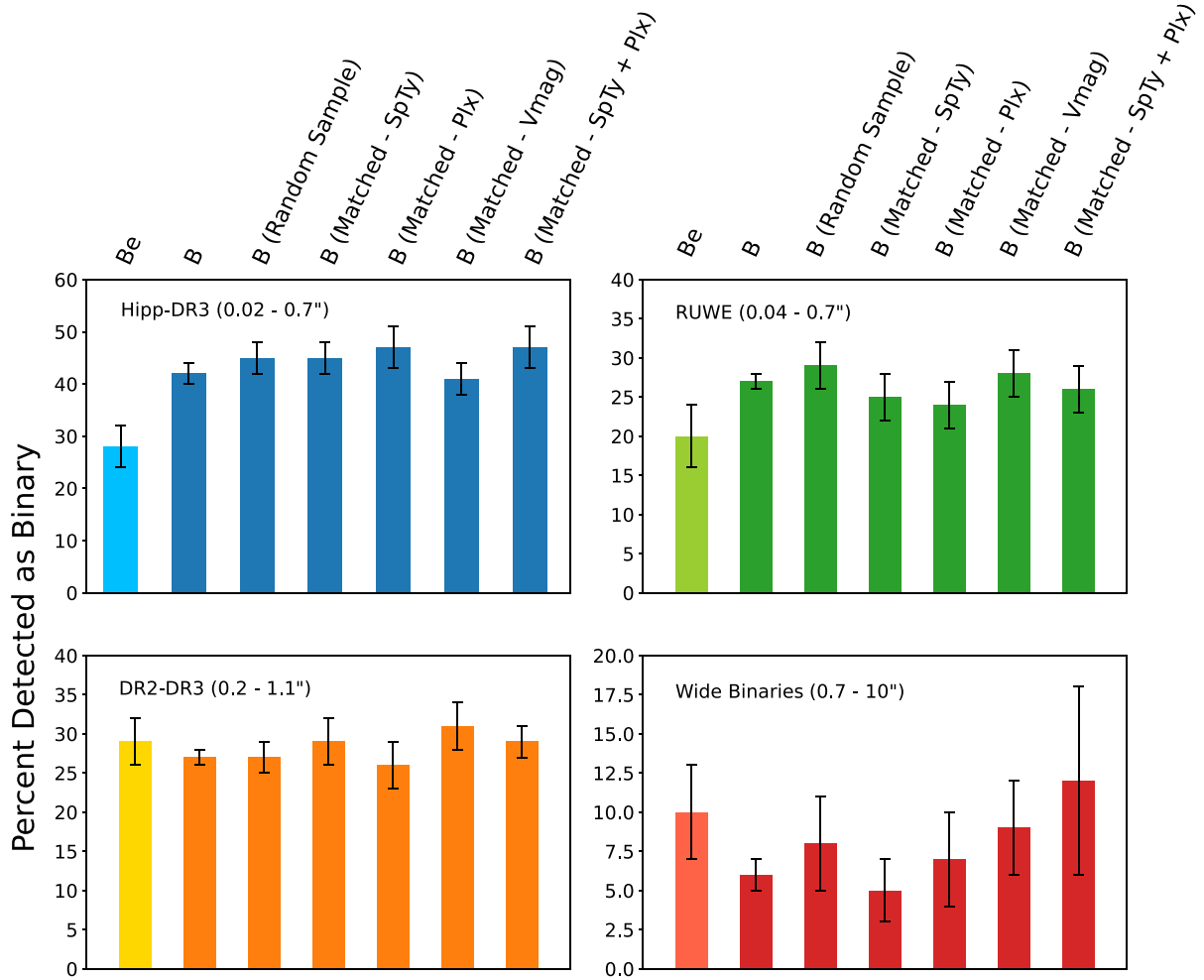


Figure 4. Summary of the binary fractions of B and Be stars, as determined by *Hipparcos–Gaia* DR3, *Gaia* DR2-DR3 PMA values, *Gaia* DR3 RUWE values, and resolved binaries (see the text). Also presented are the binary fractions of the various subsamples of the B type stars, taken in order to account for any biasing effects. ‘Matched’ here indicates that a subsample of the B stars has been created such that the distribution of a given variable in the subsample is drawn from the same parent distribution as the Be population. Note that the ‘Wide Binaries’ plot is noisier due to smaller number statistics. The *Hipparcos–Gaia* DR3 values, probing the smallest separations, show a significantly lower Be binary frequency (in each case a greater than 3σ difference), while all other approaches return similar binary fractions to within the errors. Based upon this we report a dearth of Be binaries with separations between 0.02 and 0.7 arcsec, and, as discussed in Section 3.5, we further constrain these missing binaries to between 0.02 and 0.2 arcsec.

0.1–8 arcsec, determined binary fractions of B and Be stars at 29 ± 8 and 30 ± 8 per cent. This finding could imply that the difference in the two binary fractions disappears towards larger separations.

Exploiting the added information provided by *Gaia*, we performed a basic search for spatially resolved B and Be binaries by cross-matching the sample depicted in Fig. 4, and looking for sources within a radius of 10 arcsec. Any ‘duplicate’ sources that were

retrieved were then deemed to be probable companions to the primary if they satisfied:

$$|\omega_{\text{primary}} - \omega_{\text{duplicate}}| \leq \sigma_{\text{primary},\omega} + \sigma_{\text{duplicate},\omega}, \quad (2)$$

where ω is the parallax of either star, and σ_{ω} is the uncertainty corresponding to either parallax.

Based on this basic test, 6 ± 1 per cent of B and 10 ± 3 per cent of Be V-type stars are found to have potential resolved companions within a distance of 10 arcsec. These values remained consistent even when randomly sampling or when generating semirandom samples of B stars intended to match the spectral type, parallax, or apparent magnitude distributions of the Be stars. A summary of these results can also be found in Fig. 4. In the case of each of the distribution matching samples, a Kolmogorov–Smirnov test was performed in order to verify that the distribution of each given parameter in the B star sample is likely being drawn from the same parent distribution as the Be star sample.

Presuming that these additional sources are indeed binary companions poses an interesting question. That being, why do Be stars have binary companions at a lower rate than their B type equivalents at close (i.e. <0.7 arcsec) separations, but at similar rates at greater separations?

3.5 Further constraints on binary separation

In this study we have determined, through the use of various astrometric measures, between separations of 0.02 and 0.7 arcsec, the binary fraction of Be stars is significantly lower than that of their B star equivalents, while they are similar at larger separations. Let us continue by further identifying at which separation the B binary stars become more prevalent.

Table 2 reveals that by comparing the two PMA values and looking at those systems detected by the *Hipparcos*–*Gaia* DR3 PMA but not by the *Gaia* DR2–DR3 PMA, we can constrain the lack of Be binaries to between 0.02 and 0.2 arcsec. We also note that at separations greater than 0.2 arcsec, B and Be stars have similar fractions of their populations in binary systems – in agreement with the previous most recent comparative study of these stars (Oudmaijer & Parr 2010).² Additionally, we note that the RUWE detects statistically similar rates of B and Be stars as being in binary systems. Thus, by virtue of the RUWE’s sensitivity stretching between 0.04 and 0.7 arcsec, we are able to confine the dearth of Be binaries even further – restricting them to between 0.02 and 0.04 arcsec.

4 DISCUSSION

In previous sections we have established, for the first time, ranges of angular separation and magnitude difference within which the PMA and RUWE are sensitive to binarity.

We have then used these measures to reveal a greater than 3σ dearth of Be stars in binary systems at separations unresolved by

²Although we do not wish to make quantitative comparisons between values reported by our different detection methods, a larger binary fraction detected by the *Hipparcos*–*Gaia* DR3 PMA (42 ± 2 per cent) than the *Gaia* DR2–DR3 PMA (27 ± 1 per cent) would be expected in the case of a log-flat distribution of separations (as per Öpik’s law; Öpik 1924). This is because the separation range probed by the *Hipparcos*–*Gaia* DR3 PMA (0.02 to 0.7 arcsec) is almost twice the width in log-space as that of the *Gaia* DR2–DR3 PMA (0.2 to 1.1 arcsec). Conversely, by themselves the values reported for the Be stars may indicate a distribution decreasing towards to closer separations that we are sensitive to.

Table 3. Summary of *Gaia* DR3–*Hipparcos* PMA and RUWE values for Be stars quoted in Nazé et al. (2022) as being known to host stripped companions. PMA and RUWE values marked with an asterisk (*) constitute binary detections.

Name	Spectral type	PMA	RUWE
φ Per	B1.5Ve	0.23	1.804*
HD 29441	B2.5Vne	1.17	1.125
HD 41335	B1.5IV-Ve	8.13*	1.515*
HD 43544	B3Ve	0.66	1.047
HD 51354	B3Ve	0.79	1.055
HD 58978	B0.5IVe	2.52	0.941
HD 60855	B2Ve	1.52	1.097
HD 113120	B2IVne	6.93*	2.385*
κ^1 Aps	B2Vnpe	1.48	1.060
HD 152478	B3Vnpe	1.82	0.990
HD 157832	B1.5Ve	1.60	0.735
28 Cyg	B3IVe	1.55	1.113
HD 194335	B2IIIe	3.81*	1.041
59 Cyg	B1Ve	6.38*	2.724*
60 Cyg	B1Ve	6.31*	0.142
8 Lac A	B1IVe	0.87	1.480*

Gaia, compared to B stars. We then further constrained this absence of Be binaries to separations between 0.02 and 0.04 arcsec.

These results pose a conundrum, as one might naively assume that this implies that the Be phenomenon more favourably occurs via single-star pathways, rather than the currently favoured binary pathways. Therefore, in order to continue to pursue the binary pathway for Be formation, we must consider what sort of companion will remain undetected by these methods while also remaining consistent with such models of Be formation?

In this section we will posit some explanations for this difference in binary fraction, alongside the implication for models regarding the formation of the Be phenomenon.

4.1 Stripped companions

One such solution invokes the presence of a companion whose envelope has been stripped by the putative Be star. Accretion from such a companion would provide a source for the initial spin-up mechanism that eventually results in the formation of the Be stars’ characteristic disc (El-Badry et al. 2022; Jones et al. 2022) while also allowing the companion to become low-mass, dim, or close enough to the host star (Frost et al. 2022) to be unlikely to be detected via the PMA.

Such a model has been suggested to be the route through which 20–100 per cent of field Be stars form (El-Badry & Quataert 2021), and a significant number of these stripped companions to Be stars have been reported in the literature (Bodensteiner et al. 2020b; El-Badry et al. 2022; Frost et al. 2022; see Table 3). Additionally, no close main-sequence companions to Be stars have been confirmed (Bodensteiner, Shenar & Sana 2020a), which is consistent with what would be expected in the case of a stripped companion origin for Be stars (although it should be noted that this study only considers massive Be stars – i.e. spectral types earlier than B1.5). As such, they may be responsible for hydrogen-poor supernovae and neutron star mergers resulting in gravitational wave sources.

The periods proposed to be required in order for stripping to begin by Han et al. (2002) are of order 0.1–10 d for Common Envelope Ejection and 400–1500 d for Roche Lobe Overflow. Using the average distance to the Be stars in our sample (~ 260 pc), and

assuming a circular, Keplerian orbit, these stars would require a binary companion at a separation of 0.02 arcsec (approximately 5 au) or closer in order for stripping to initiate. While the process of mass transfer would then act to widen the orbit of this companion, the resultant stripped star would be low-mass and faint. We would thus expect that the majority of stripped companions, if they indeed exist, would be missed by both our PMA values and the RUWE as they will too close to the host Be star, or too low-mass and dim to be detected.

In support of this, PMA and RUWE values were obtained for 13 Be stars confirmed via UV observations to host a stripped companion and 3 Be stars with low mass companions detected via radial velocity shifts (all of those from Nazé et al. 2022). In order for the above suggestion to have any validity, these stars, which are known to host stripped companions, should not be detected as binaries using the measures detailed within this paper. A summary of these objects and their *Gaia* data can be found in Table 3.

Seven of these 16 systems are detected by either method; five by the *Hipparcos–Gaia* DR3 PMA, and five by the RUWE, with three objects detected by both. However, five of these seven detected systems (the exceptions being HD 194 335 and HD 200310) have known additional companions (Mason et al. 2022) at separations within the range the PMA’s and RUWE are sensitive to. In addition, these companions are at separations significantly larger than required for the periods reported by Nazé et al. (2022), and are therefore inconsistent with being the reported stripped companion. An undetected, third, companion has also been suggested in the case of HD 200 310 to explain the eccentric orbit of the stripped companion (Klement et al. 2022), making the system a potential triple. Thus, the true fraction of detected stripped companions would seem to be either 6 or 12 per cent depending on how one wishes to treat the case of HD 200310. Therefore, we reach the conclusion that the stripped companions listed in Nazé et al. (2022) are by and large not detected by the PMA or RUWE, whose detections turn out to trace a third body in these systems instead. Thus, the potential for the Be phenomenon being caused by the presence of stripped companions remains consistent with our results.

4.2 Triples

Intriguingly, the separation range of the ‘missing’ Be binaries (0.02–0.04 arcsec; with 0.02 arcsec corresponding to 5 au) is typically too large for mass transfer to have occurred (typically less than 4 au is required per the periods reported in Han et al. 2002). The natural next question to ask is then, why would the Be stars lack binaries in this particular separation range, while the stripping of a close companion should occur at smaller separations?

A clue can be found in the fact that the systems listed in Table 3 show a high incidence rate of higher order multiplicity, with 56 ± 18 per cent of this sample of Be stars known to host a stripped companion having additional companions (Mason et al. 2022) at separations larger than those reported in Nazé et al. (2022). Additionally this number is also somewhat elevated with the expected incidence rate of higher order multiplicity posited by Moe & Di Stefano (2017) – being around 40 per cent.

The presence of such a third companion can neatly explain the absence of detected Be binaries at larger separations, while also allowing for any companion stars to become close enough for mass transfer to occur; it is well known that higher order multiplicity can result in the hardening of an inner binary. Indeed, a third body increases the occurrences of migration and eventual binary

interactions significantly (Toonen, Boekholt & Portegies Zwart 2022; Kummer, Toonen & de Koter 2023).

Recent models (Preece et al. 2022) suggest that of the systems that eventually form stripped companions – half form via binary pathways and half form via triple pathways. This can take place by either mass transfer occurring within the inner binary – with the outer tertiary star potentially becoming unbound – or a merger of the inner binary and mass transfer occurring between the two remaining stars (Preece et al. 2022).

Our results therefore imply that close binary interactions are responsible for the formation of Be stars, which constitute 20 per cent of the B star population, with a migratory effect causing the lack of Be binaries in the 0.02 to 0.04 arcsec. Moreover, we suggest that triplicity must play a vital role in triggering this migration, and thus in the formation of Be stars as a whole.

4.3 Potential limitations of the methods

We will now address the various potential limitations of the methods as described in Sections 2 and 3.

4.3.1 Sample selection

First, we note that the Be phenomenon is known to be transient, with the disc known to disappear and reappear on short time-scales, which can lead to the potential misclassification of Be stars as B stars (Rivinius, Carciofi & Martayan 2013). Thus, contamination of the B star sample with misclassified Be stars could effect the previously detected binary fractions for the B star sample. However, as the Be sample should have low contamination (as observation of the emission-line features associated with the Be phenomenon is required for classification as a Be star, even if these features later disappear), the detected Be binary fractions should be representative of the Be population as a whole – and thus representative of any misclassified Be stars. Therefore, should there be a significant amount of Be contaminants in the B star sample, then they will act to bring the true B binary fraction down – thus the true B binary fraction would differ more significantly from the Be fraction.

We also note that, as this sample is selected from the BSC (Hoffleit & Jaschek 1982; Hoffleit & Jaschek 1991), these stars are necessarily bright. While *Gaia* astrometric fits become systematic dominated at $G < 13$ (Lindgren 2020), the resultant increase in uncertainties associated with this effect ensures that the PMA is still a viable metric – as a signal-to-noise ratio is used to quantify binary detection. Additionally, in the calculation of the new *Gaia* DR2-DR3 PMA’s corrections to the respective proper motions of bright stars as proscribed by Lindgren et al. (2018) and Cantat-Gaudin & Brandt (2021) have been applied. Steps have also been taken to ensure that the two samples are subject to the same selection effects, and these are detailed in Section 3.3, thus any systematic effects should be consistent between the two samples. To check this, all stars brighter than 5 mag were removed from the B and Be samples, which resulted in zero change to the reported dearth of Be binaries within the 0.02–0.2 arcsec range.

4.3.2 Variability

While photometric variability has not been quantitatively considered here, we anticipate that it is unlikely to effect the PMA unless the variability is occurring both asymmetrically and on a scale similar to the sensitive separation range, here we look at this in more detail.

First, consider a single star exhibiting symmetrical variation; in this case the position of the photocentre does not deviate from the centre of mass – thus leading to no PMA. When we then introduce an unresolved companion, the position of the photocentre therefore deviates from the position of the centre of mass; however the magnitude of the deviation varies with the variability cycle. Thus, while such variability should not produce a false positive detection of binarity, it is possible for it to induce a false negative. The likelihood of this false negative thus depends on two factors: the magnitude of the variability, and the time-scale on which it occurs (as observations taken at the same point in the variability cycle will obviously be unaffected, and variability with a period shorter than either individual observing period will be smeared, diminishing the effect on the PMA).

In the case of asymmetric variability – i.e. that caused by phenomena such as mass ejection, or variations in surface brightness in stars such as red super-giants (Chiavassa et al. 2022), or asymmetry within a disc (Meilland et al. 2007; Stee et al. 2013) – deviation of the photocentre from the centre of mass will occur. However, such asymmetry would have to be on a similar scale to the PMA’s sensitive range in order for such deviation to be construed as a false positive detection of binarity.

In the specific case of this study, we anticipate little effect of the photometric variability of Be stars (Labadie-Bartz et al. 2017, 2022) on our PMA values. This is due to the observed periods of Be variability being significantly shorter than the observing periods of *Gaia* DR2, DR3, and *Hipparcos* (668, 1038 and 1227 d, respectively), with the longest period variability found by Labadie-Bartz et al. (2017) being approximately 200 d. Similarly, variability caused by mass-loss on to the Be disc is unlikely to significantly effect the PMA, as the discs of Be stars, with sizes of order milli-arcseconds, are very small when compared to the resolution achieved by *Gaia* DR3 (i.e. 0.7 arcsec; Quirrenbach et al. 1997; Wheelwright et al. 2012). Additionally, by similar logic, asymmetry of the discs themselves (Meilland et al. 2007; Stee et al. 2013) is also expected to have little effect on the PMA measurements of these stars. Likewise, the stars are necessarily smaller than their disc, they are expected to be too small to have asymmetric surface brightness that would effect the PMA.

5 CONCLUSIONS

In this paper we have performed the largest scale comparative study of B and Be star binarity to date, utilizing both the *Hipparcos–Gaia* DR3 PMA values found in Kervella, Arenou & Thévenin (2022) and new *Gaia* DR2-DR3 PMA values calculated for the first time here, alongside the *Gaia*-provided RUWE.

We evaluate the limits in which these methods are sensitive to binarity. Particularly we determine for the first time the range of angular separations they are capable of reliably detecting, through the use of WDS (Mason et al. 2022) data. We thus find that the *Hipparcos–Gaia* DR3 and *Gaia* DR2-DR3 PMA’s are sensitive to binaries with separations in the 0.02–0.7 arcsec and 0.2–1.1 arcsec ranges, respectively. Likewise the RUWE is found to be sensitive to separations between 0.04 and 0.7 arcsec.

Through the use of these astrometric methods in combination with one another, we report a greater than 3σ dearth of Be binaries compared to B stars at separations between 0.02 and 0.2 arcsec, with the fractions of B and Be stars found to be in binary systems at these separations being 28 ± 1 and 17 ± 3 per cent, respectively.

We posit that this apparent lack of Be binaries provides evidence for the presence of stripped companions to the Be stars, with the mass-transfer process by which they are created having been previously

suggested as an origin for the Be phenomenon. Such stars would go undetected by the measures used within this paper, as they are too close, low-mass, and dim to induce a significant enough deviation of the photocentre from the centre of mass. We also find that Be stars previously reported to have a stripped companion have additional companions (i.e. triples and higher order multiples) at a rate somewhat elevated from the expected rate for B stars as a whole. Therefore, we suggest that migration of binary companions to Be stars to separations at which mass-transfer can occur, triggered by a third companion, must play an important role in the formation of Be stars.

ACKNOWLEDGEMENTS

The STARRY project has received funding from the European Union’s Horizon 2020 research and innovation programme under MSCA ITN-EID grant agreement No 676036. This project has also received funding from the European Union’s Framework Programme for Research and Innovation Horizon 2020 (2014-2020) under the Marie Skłodowska-Curie Grant Agreement No. 823734. This work has used data from the European Space Agency (ESA) mission *Gaia* (<https://www.cosmos.esa.int/gaia>), processed by the *Gaia* Data Processing and Analysis Consortium (DPAC, <https://www.cosmos.esa.int/web/gaia/dpac/consortium>). Funding for the DPAC has been provided by national institutions, in particular the institutions participating in the *Gaia* Multilateral Agreement.

DATA AVAILABILITY

The catalogues of the proper motion anomalies and RUWE values of both the sample of B and Be stars, as well as the WDS binaries are available from the corresponding author on reasonable request, and will also be made available via VizieR.

REFERENCES

- Abt H. A., Cardona O., 1984, *ApJ*, 285, 190
 Abt H. A., Levy S. G., 1978, *ApJS*, 36, 241
 Belokurov V. et al., 2020, *MNRAS*, 496, 1922
 Bodenheimer P., 1995, *ARA&A*, 33, 199
 Bodensteiner J., Shenar T., Sana H., 2020a, *A&A*, 641, A42
 Bodensteiner J. et al., 2020b, *A&A*, 641, A43
 Boubert D., Evans N. W., 2018, *MNRAS*, 477, 5261
 Brandt T. D., 2018, *ApJS*, 239, 31
 Brandt T. D., 2021, *ApJS*, 254, 42
 Cantat-Gaudin T., Brandt T. D., 2021, *A&A*, 649, A124
 Chiavassa A., Kudritzki R., Davies B., Freytag B., de Mink S. E., 2022, *A&A*, 661, L1
 Draper Z. H., Wisniewski J. P., Bjorkman K. S., Meade M. R., Haubois X., Mota B. C., Carciofi A. C., Bjorkman J. E., 2014, *ApJ*, 786, 120
 El-Badry K., Quataert E., 2021, *MNRAS*, 502, 3436
 El-Badry K., Rix H.-W., Heintz T. M., 2021, *MNRAS*, 506, 2269
 El-Badry K. et al., 2022, *MNRAS*, 516, 3602
 Frost A. J. et al., 2022, *A&A*, 659, L3
 Gaia Collaboration, 2018, *A&A*, 616, A1
 Gaia Collaboration, 2021, *A&A*, 649, A1
 Gaia Collaboration, 2023, *A&A*, 674, A1
 Granada A., Ekström S., Georgy C., Krtićka J., Owocki S., Meynet G., Maeder A., 2013, *A&A*, 553, A25
 Griffiths S. C., Hicks R. B., Milone E. F., 1988, *J. R. Astron. Soc. Can.*, 82, 1
 Han Z., Podsiadlowski P., Maxted P. F. L., Marsh T. R., Ivanova N., 2002, *MNRAS*, 336, 449
 Hastings B., Wang C., Langer N., 2020, *A&A*, 633, A165

Hastings B., Langer N., Wang C., Schootemeijer A., Milone A. P., 2021, *A&A*, 653, A144

Hoffleit D., Jaschek C., 1982, The Bright Star Catalogue. Fourth revised edition. (Containing data compiled through 1979). Yale University Observatory, New Haven

Hoffleit D., Jaschek C., 1991, The Bright Star Catalogue, 5th ed. Yale University Observatory, New Haven, Conn.

Jones C. E. et al., 2022, *Astrophys. Space Sci.*, 367, 124

Kervella P., Arenou F., Mignard F., Thévenin F., 2019, *A&A*, 623, A72

Kervella P., Arenou F., Thévenin F., 2022, *A&A*, 657, A7

Klement R. et al., 2019, *ApJ*, 885, 147

Klement R. et al., 2022, *ApJ*, 926, 213

Kummer F., Toonen S., de Koter A., 2023, *A&A*, 678, A60

Labadie-Bartz J. et al., 2017, *AJ*, 153, 252

Labadie-Bartz J., Carciofi A. C., Henrique de Amorim T., Rubio A., Luiz Figueiredo A., Ticiani dos Santos P., Thomson-Paessant K., 2022, *AJ*, 163, 226

Lindgren L., 2020, *A&A*, 633, A1

Lindgren L. et al., 2018, *A&A*, 616, A2

Lindgren L. et al., 2021, *A&A*, 649, A2

Mason B. D., Wycoff G. L., Hartkopf W. I., Douglass G. G., Worley C. E., 2001, *AJ*, 122, 3466

Meilland A. et al., 2007, *A&A*, 464, 73

Moe M., Di Stefano R., 2017, *ApJS*, 230, 15

Nazé Y., Rauw G., Smith M. A., Motch C., 2022, *MNRAS*, 516, 3366

Öpik E., 1924, Publ. Tartu Astrofizica Obs., 25, 1

Oudmaijer R. D., Parr A. M., 2010, *MNRAS*, 405, 2439

Oudmaijer R. D., Jones E. R. M., Vioque M., 2022, *MNRAS*, 516, L61

Owocki S., Cranmer S., 2002, in Aerts C., Bedding T. R., Christensen-Dalsgaard J., eds, ASP Conf. Ser. Vol 259, IAU Colloq. 185: Radial and Nonradial Pulsations as Probes of Stellar Physics. Astron. Soc. Pac., San Francisco, p. 512

Penoyre Z., Belokurov V., Evans N. W., 2022, *MNRAS*, 513, 2437

Pineau F.-X., Boch T., Derrière S., Schaaff A., 2020, in Ballester P., Ibsen J., Solar M., Shorridge K., eds, ASP Conf. Ser. Vol. 522, Astronomical Data Analysis Software and Systems XXVII. Astron. Soc. Pac., San Francisco, p. 125

Porter J. M., Rivinius T., 2003, *PASP*, 115, 1153

Preece H. P., Hamers A. S., Battich T., Rajamuthukumar A. S., 2022, *MNRAS*, 517, 2111

Quirrenbach A. et al., 1997, *ApJ*, 479, 477

Rivinius T., Carciofi A. C., Martayan C., 2013, *A&AR*, 21, 69

Semaan T., Hubert A. M., Zorec J., Gutiérrez-Soto J., Frémat Y., Martayan C., Fabregat J., Eggenberger P., 2018, *A&A*, 613, A70

Shao Y., Li X.-D., 2014, *ApJ*, 796, 37

Stassun K. G., Torres G., 2021, *ApJ*, 907, L33

Stee P. et al., 2013, *A&A*, 550, A65

Suffak M., Jones C. E., Carciofi A. C., 2022, *MNRAS*, 509, 931

Toonen S., Boekholt T. C. N., Portegies Zwart S., 2022, *A&A*, 661, A61

Townsend R. H. D., Owocki S. P., Howarth I. D., 2004, *MNRAS*, 350, 189

Van Leeuwen F., 2007, *A&A*, 350

Wheelwright H. E., Bjorkman J. E., Oudmaijer R. D., Carciofi A. C., Bjorkman K. S., Porter J. M., 2012, *MNRAS*, 423, L11

Wisniewski J. P., Draper Z. H., Bjorkman K. S., Meade M. R., Bjorkman J. E., Kowalski A. F., 2010, *ApJ*, 709, 1306

Zorec J. et al., 2016, *A&A*, 595, A132

Zorec J. et al., 2017, *A&A*, 602, A83

APPENDIX: DERIVATION OF THE THEORETICAL LIMITS OF THE PMA

In order to obtain a theoretical, lower bound binary separation detectable via the PMA, it is easiest to consider a simple binary system. Take, for example, a system of two intermediate-mass (i.e. $2\text{--}5M_{\odot}$) main-sequence stars in a circular orbit. In such a system, where both stars are of a known mass, the centre of mass is easily

derivable. Likewise, by applying the mass–luminosity relationship

$$\frac{L}{L_{\odot}} \simeq 1.4 \frac{M}{M_{\odot}}^{3.5} \quad (\text{A1})$$

for such stars, as given by Griffiths, Hicks & Milone (1988), the location of the photocentre is similarly able to be determined.

The minimum theoretically detectable separation will occur for a system where (a) the difference between the centre of mass and the photocentre is at a maximum and (b) where the change in absolute orbital phase is at a maximum (i.e the observations are spaced half an orbit apart).

The latter of these criteria (b) is fairly easy to evaluate, provided we know the masses of the two stars. However, we must first evaluate the former criteria (a) in order to determine the mass ratio at which the largest offset between the photocentre and centre of mass is achieved. This proves to be a somewhat more involved process.

By normalizing the separation between the two stars to 1, it is possible to write the photocentre and centre of mass equations as

$$a_{1,M/L} + a_{2,M/L} = 1 \quad (\text{A2})$$

$$M_1 a_{1,M} = M_2 a_{2,M} \quad (\text{A3})$$

$$L_1 a_{1,L} = L_2 a_{2,L} \quad (\text{A4})$$

$$\delta = |a_{1,M} - a_{1,L}|, \quad (\text{A5})$$

where $a_{1/2,ML}$ is the separation of the primary (1) or secondary (2) companion from the centre of mass (M) or photocentre (L) depending on the subscript, M is the mass of an individual star, L is the corresponding luminosity, and δ is the offset between the centre of mass and the photocentre.

From this set of equations, alongside the mass–luminosity relation given by equation (A1), it is possible to rewrite equations (A3) and A4 in terms of $a_{1,ML}$ and the mass ratio of the two stars, M_1/M_2 , giving the expression of δ as

$$\delta = \left| \frac{M_2^{3.5}}{M_1} \left(\frac{M_2}{M_1} + 1 \right)^{-1} - \frac{M_2}{M_1} \left(\frac{M_2}{M_1} + 1 \right)^{-1} \right| \quad (\text{A6})$$

By taking the derivative of this with respect to the mass ratio, and solving for $d\delta/d(\frac{M_1}{M_2}) = 0$, it is possible to obtain the mass ratio for which the maximum offset between the centre of mass and photocentre is achieved. This is found to occur for a mass ratio, $M_1/M_2 = 0.47$ for intermediate-mass main-sequence stars.

If we now assume a circular orbit with a stationary centre of mass, then the photocentre motion is resultant entirely from the orbital motion of the system. Thus, as the maximum change in proper motion occurs for observations separated by $\frac{3n+1}{2}$ orbital periods, where n is some integer greater or equal to zero, in this case resulting in the change in proper motion being twice the instantaneous proper motion. Thus, we can simply express this change in proper motion, $\Delta\mu$ as

$$\Delta\mu = 2\mu_{st} = 2\omega r \delta = \frac{4\pi r}{P} \delta, \quad (\text{A7})$$

where μ_{st} is the short-term proper motion measurement, which here can be reduced to the tangential velocity of the photocentre. P is the period of the orbit and r is the binary separation.

While this approximation of the relation between the change in proper motion and the period of a binary system may seem to imply that the proper motion changes increasingly towards shorter

period binaries, this approximation ignores the effects of smearing on the actual observational data. In reality this smearing across the observational timeframe causes a drop in sensitivity at shorter periods (Kervella, Arenou & Thévenin 2022), with the maximum sensitivity being achieved for periods similar to twice that of the time elapsed between the two observations. Here, this resolves to a period of ≈ 50 yr for the *Hipparcos*–*Gaia* DR3 PMA, and ≈ 1 yr in the case of the *Gaia* DR2–DR3 PMA.

Using this calculated PMA, in concert with standard errors for the three surveys in question [in this case the *Hipparcos* re-reduction (Van Leeuwen 2007) and the *Gaia* DR2 and 3 (Lindegren et al. 2018, 2021) although other values can be used as and where appropriate], a lower limit of separation can be obtained. This is achieved via propagating the standard errors through the calculations required to determine the PMA (as detailed in Kervella, Arenou & Thévenin 2022) and using this to generate a signal-to-noise ratio. As we have an expression for the change in proper motion that is a function of the separation we can thus write

$$\frac{\Delta\mu}{N} = \frac{2\pi r}{NP} \delta, \quad (\text{A8})$$

where N is the standard error of calculating the PMA. Thus, by setting the above to equal the Kervella, Arenou & Thévenin (2022) defined detection threshold of 3, and solving for r we arrive at a theoretical minimum binary separation detectable by the PMA. In the case of the PMA obtained from *Hipparcos* re-reduction and *Gaia* DR3 data this lower limit is estimated to be 0.01 arcsec, and in the case of the *Gaia* DR2–DR3 PMA this is 0.0025 arcsec. However the effect of the observational smearing is underestimated, particularly in the case of the *Gaia* DR2–DR3 PMA, where the PM measurement period covers the entirety of long-term proper motion’s timeframe – likely resulting in less sensitivity to small separations than predicted here.

This paper has been typeset from a $\text{\TeX}/\text{\LaTeX}$ file prepared by the author.